Journal of Environmental Management 410 (2026) 130075

Contents lists available at ScienceDirect

Journal of Environmental Management

journal homepage: www.elsevier.com/locate/jenvman

Research article

Technical feasibility of adding 20% wind turbine blade waste to concrete: Fresh, mechanical, deformational, and sustainability assessment

Víctor Revilla-Cuesta [a], Javier Manso-Morato [a,*], Ana B. Espinosa [b], Marta Skaf [b]

[a] Department of Civil Engineering, Escuela Politécnica Superior, University of Burgos, c/ Villadiego s/n, Burgos, 09001, Spain
[b] Department of Construction, Escuela Politécnica Superior, University of Burgos, c/ Villadiego s/n, Burgos, 09001, Spain

ARTICLE INFO

Keywords:
Concrete
Wind turbine blade
Glass fiber-reinforced polymer
Mechanical property
Energy absorption
Life cycle assessment

ABSTRACT

The recycling and valorization of decommissioned wind turbine blades represent a pressing environmental challenge. This study explores a recycling route in which the blades were not selectively crushed, thus yielding Wind Turbine Blade Waste (WTBW) composed of balsa wood, polymers, and fibers and microfibers from Glass Fiber-Reinforced Polymer (GFRP). This by-product was subsequently incorporated as a partial replacement (20% by volume) of natural aggregates in concrete. The fresh, mechanical, deformational, and sustainability performance of the resulting concrete was evaluated. 20% WTBW inclusion slightly reduced workability, though concrete maintained a slump class S2 thank empirical adjustment of water and plasticizer contents, in principle ensuring placement by conventional vibration. Mechanical properties were generally reduced due to the weak particles in WTBW. Nevertheless, flexural strength was preserved (5.59 MPa) owing to the three-dimensional reinforcement of the GFRP fibers. Such fiber network also enhanced post-failure performance, doubling the absorbed energy under bending and promoting more ductile failure modes characterized by reduced crack width and absence of surface spalling. Scanning electron microscopy confirmed a proper orientation and crack stitching of GFRP microfibers, which also contributed to this improvement. A cradle-to-gate life cycle assessment showed reductions of approximately 6% in both abiotic depletion potential for fossil fuels and global warming potential, both in total terms and per unit of strength or absorbed energy under bending. These results, statistically validated by an analysis of variance, indicate that concrete incorporating 20% WTBW could, in theory, be sustainably used in elements with reduced mechanical requirements and predominantly bending stresses.

1. Introduction

In a global context where the fight against climate change is a priority across all productive sectors, renewable energies have become key elements in the generation of clean energy and the reduction of greenhouse gas emissions (Mohamad and Ab-Rahim, 2025). Among them, wind energy stands out as one of the most prominent and widely adopted renewable sources, having experienced significant growth in recent years (Global Wind Energy Council (GWEC), 2025). Global installed wind power capacity increased from approximately 17 GW in the year 2000 to around 1140 GW in 2024, enabling the generation of 8.1% of the world's electricity (approximately 2494 TWh) (World Wind Energy Association (WWEA), 2025). In 2024 alone, 117 GW of new capacity were installed, representing an annual growth rate of approximately 11.5% (World Wind Energy Association (WWEA), 2025). Forecasts indicate that the average annual growth rate will remain around 8.8% until 2030 (Global Wind Energy Council (GWEC), 2025). Within this context, the countries with the highest installed wind power capacity are China (520 GW), the United States (154 GW), Germany (73 GW), India (48 GW), Brazil (34 GW), and Spain (31 GW) (Global Wind Energy Council (GWEC), 2025). Notably, China accounted for nearly three-quarters of new installations in 2024, although global efforts are underway to promote wind energy development in other countries as well (Asociación Empresarial Eólica (AEE), 2024).

The operational lifespan of a wind turbine typically ranges from 20 to 25 years, point at which maintenance costs become excessively high relative to the amount of electricity generated, rendering their operation economically unviable (Li et al., 2026). At this stage, turbines are generally either decommissioned or repowered, that is, replaced with newer, higher-capacity models (Safaei et al., 2022). Currently, the earliest generations of wind turbines are reaching the end of their service life. As time progresses, the number of turbines requiring decommissioning is expected to increase significantly due to the continuous

* Corresponding author.
E-mail address: jmanso@ubu.es (J. Manso-Morato).

https://doi.org/10.1016/j.jenvman.2026.130075
Received 7 April 2026; Received in revised form 10 May 2026; Accepted 24 May 2026
Available online 27 May 2026

Acronyms:

abiotic depletion potential for fossil fuels (ADPf)
analysis of variance (ANOVA)
glass fiber-reinforced polymer (GFRP)
global warming potential (GWP)
interfacial transition zones (ITZ)
life cycle assessment (LCA)
life cycle inventory (LCI)
wind turbine blade waste (WTBW)

annual growth in installed wind power capacity (World Wind Energy Association (WWEA), 2025). The decommissioning of these turbines has highlighted the need to manage, recycle, and recover value from their various components, ensuring that the environmental benefits of wind energy are not offset by negative impacts associated with end-of-life waste (Das Karmakar and Chattopadhyay, 2025). While the metallic components of wind turbines pose little difficulty due to their well-established recycling processes, the blades are a significant challenge (Liu and Barlow, 2017).

These end-of-life wind turbine blades are mainly composed of Glass Fiber-Reinforced Polymer (GFRP), made up of glass fibers bonded within an epoxy resin matrix. This material provides high tensile strength while maintaining relatively low weight (Menna et al., 2025). However, if the entire blade were constructed solely from GFRP, its overall weight would be excessive, and the blade-to-nacelle connection would be subjected to extremely high mechanical stresses (Li et al., 2025). To mitigate this, GFRP is alternated with balsa wood, a lightweight yet strong material, in areas of the blade where mechanical stresses are lower (Borrega and Gibson, 2015). In addition, blades incorporate various polymers that serve multiple functions, including internal stiffening elements, external protective gel coatings, and adhesive bonding agents, among others (Joustra et al., 2021a). This complex composition significantly complicates the management of the end-of-life wind turbine blades process, although several circular economy-based solutions have been addressed (Fonte and Xydis, 2021; Tao et al., 2023; Nagle et al., 2022).

One potential strategy is the reuse and repurposing of decommissioned wind turbine blades. In this approach, blades can be sectioned and processed into construction elements that may be used in applications such as playground structures, shelters, or urban furniture (Nagle et al., 2022). Overall, promising results have been reported to extend the service life of blade materials while preserving their favorable mechanical properties (Johst et al., 2025; Ramaswamy et al., 2025a). However, several aspects need to be considered. First, the geometry and material heterogeneity of wind turbine blades strongly influence the feasibility and suitability of each derived structural component (Joustra et al., 2021a). Second, structural monitoring of the repurposed elements is essential to ensure adequate performance throughout their service life, particularly under variable loading conditions (Henao et al., 2024; Ramaswamy et al., 2025b). Finally, surface treatments are typically required to prevent user exposure to sharp glass fibers embedded in the GFRP and to mitigate degradation of the epoxy matrix due to UV radiation and moisture ingress (Joustra et al., 2021b). The implementation of this strategy for end-of-life blade management would benefit from incorporating greater modularity into wind turbine blade design, facilitating disassembly (Nagle et al., 2022; Joustra et al., 2021b).

Another possibility is the recycling of wind turbine blades by processing their individual components (GFRP, wood, and polymers) separately (Yazdanbakhsh et al., 2018). This separation can be achieved either chemically or thermally, by degrading the polymers that bind the different materials, or mechanically, through cutting. The former approach is generally not environmentally sustainable, as it still requires a solution for managing the waste from polymers' removal (Rani et al., 2021). The latter, while more environmentally friendly, does not allow for a fully precise separation of components (Fonte and Xydis, 2021). Once separated, the wood and polymer fractions can be incinerated, a process that, although not environmentally ideal, enables the recovery of energy through electricity generation (Liu et al., 2025a), while the isolated GFRP can subsequently be treated using two main approaches:

- One approach involves separating the individual components of the GFRP itself, allowing the recovery of the glass fibers embedded within the epoxy matrix for potential reuse. To achieve this, the epoxy matrix has to be removed, either by chemical dissolution (Shen et al., 2023) or thermal degradation (incineration) (Xu et al., 2023). However, both methods present significant drawbacks: the first one generates waste that is difficult to manage, while the second one releases greenhouse gases (Wei and Hadigheh, 2022). Additionally, the recovered glass fibers generally exhibit inferior mechanical properties compared to their original state (Rafay et al., 2024). For these reasons, ongoing research is focused on optimizing these processes to achieve the best possible outcomes in terms of minimizing environmental impact and improving the quality of the recovered glass fibers (Wei and Hadigheh, 2024).
- Another possibility is the mechanical recycling of GFRP, as this material can be machined or crushed to produce elements of regular shapes (Yazdanbakhsh et al., 2018), powder (Wu et al., 2024), or GFRP fibers (DarvishaliNezhad et al., 2026) without the need to remove the epoxy resin. These recycled elements can be used as raw materials in cement-based materials, either as a replacement for aggregates or as substitutes for conventional steel or polypropylene fibers, leveraging their high mechanical strength (Tao et al., 2023). This approach not only adds value to GFRP waste but also reduces the environmental impact associated with the extraction of natural resources required for producing these construction materials (Manso-Morato et al., 2025a). However, the use of GFRP elements as aggregates has not led to satisfactory performance, primarily due to debonding under load caused by the formation between the GFRP and the cementitious matrix of low-quality Interfacial Transition Zones (ITZ) (Yazdanbakhsh et al., 2018). Similarly, the incorporation of GFRP powder has resulted in increased porosity within the matrix, which in turn leads to decreased mechanical strength and durability (Pławecka et al., 2021). Conversely, GFRP fibers have demonstrated favorable performance. They effectively bridge the cement matrix, thereby reducing crack propagation and shrinkage, and enhancing flexural strength, impact resistance, and energy absorption capacity (Guo et al., 2025; Zhang et al., 2024). In particular, macrofibers (with an average length of approximately 47 mm) have shown great potential to improve the ductility of concrete (Xu et al., 2022).

This approach, based on the individual recycling of the components of wind turbine blades, presents the limitation that it cannot address blade recycling in an integral manner (Fonte and Xydis, 2021). Additionally, it is associated with a significant environmental impact due to the incineration of polymers and balsa wood (Wei and Hadigheh, 2022). Consequently, an alternative line of research has emerged that focuses on the mechanical recycling of the entire blade simultaneously for use as a concrete's raw material. In this method, the GFRP is crushed, along with the balsa wood and the polymers with which it is combined (Revilla-Cuesta et al., 2023). The resulting product is a mixed Wind Turbine Blade Waste (WTBW), composed of semi-spherical particles of polymers and balsa wood and GFRP fibers (Revilla-Cuesta et al., 2023). Previous studies have demonstrated the feasibility of incorporating this waste into concrete as an overall addition. At this level, the GFRP fibers stitch the matrix, improving flexural behavior without significantly compromising compressive strength (Revilla-Cuesta et al., 2024a), while also increasing ductility and energy absorption capacity (Ortega-López et al., 2024), and reducing shrinkage (Trento et al.,

2024). Simultaneously, the balsa wood and polymer particles act as lightweight aggregates, contributing to a reduction in the overall density of the mix without creating critical failure initiation points under load (Revilla-Cuesta et al., 2024b).

The research group to which the authors belong has previously investigated the replacement of up to 10% of natural aggregate with WTBW in earlier studies. These investigations addressed fresh-state and mechanical behavior (Manso-Morato et al., 2025b), the microstructural characteristics of the ITZ (Manso-Morato et al., 2025c), durability in terms of water transport and dimensional stability (Manso-Morato et al., 2026), and sustainability aspects (Manso-Morato et al., 2025b). The results obtained with 10% WTBW were satisfactory, although, from this content, the increased water demand required to maintain workability, together with the higher concentration of wood and polymer particles, appeared to begin causing more noticeable performance reductions (Manso-Morato et al., 2025b, 2025c).

Following on from that previous research, this study investigates the behavior of a conventional concrete incorporating 20% by volume of mixed WTBW as a replacement for natural aggregate, and compares it with a reference mix produced without this waste. Following the best of the authors' knowledge, no previous research in the literature has explored the impact as a whole of such high contents of mixed WTBW in concrete. The mechanical and deformational behavior, as well as the failure mechanisms at both meso- and micro-scale, are evaluated for concrete containing this high level of WTBW. Furthermore, the environmental performance of concrete is also assessed through Life Cycle Assessment (LCA). The objective is to determine whether this type of concrete could be suitable for specific applications based on the analyzed properties. Ultimately, the aim is to develop a concrete mix that performs adequately while enabling the utilization of large quantities of this waste, thereby proposing a viable valuation pathway for the significant number of wind turbine blades currently lacking a widely accepted recycling solution.

2. Materials and methods

2.1. Raw materials

The conventional raw materials used in concrete production were those available in the geographical area where the study was conducted. CEM II/A-L 42.5 R cement was employed, which is a cement type included in the standard EN 197-1 (Euronorm, 2026) that incorporates between 6% and 20% limestone as a partial clinker replacement in order to reduce cement's carbon footprint (Sim et al., 2025). Tap water from the local supply network, plasticizers, siliceous aggregate divided into three fractions (12-22 mm, 4-12 mm, and 0-4 mm), and a 0-2 mm limestone sand were also used. The density and water absorption of the aggregates were measured according to EN 1097-6 (Euronorm, 2026) and are shown in Table 1, with all values falling within typical ranges (EC-2, 2010). Additionally, their particle size distributions, determined as per EN 933-1 (Euronorm, 2026), are presented in Fig. 1. A continuous and well-graded distribution, suitable for concrete production (EC-2, 2010), was always achieved.

The mixed WTBW was obtained through the raw shredding of wind turbine blades. For this purpose, decommissioned blades were cut into approximately rectangular pieces measuring 20-30 cm per side. Without separating their components (GFRP, balsa wood, and polymers), they were subjected to crushing using a knife mill, followed by sieving with a 10 mm mesh size. The elements retained in the sieve were crushed and sieved again. The resulting waste material, shown in Fig. 2a, had an overall density of 1.63 kg/dm^3 and a bulk density of approximately 247 kg/m^3. It was formed by GFRP fibers (Fig. 2b), consisting of elongated GFRP strips; GFRP microfibers (Fig. 2c), consisting mainly of glass fibers with small fragments of epoxy resin adhered to them; balsa wood particles (Fig. 2d); polymeric fragments (Fig. 2e); and other particles that could not be mechanically separated. The proportions and size of each component are presented in Table 2. Further details on the characteristics of this WTBW can be found in previous publications (Revilla-Cuesta et al., 2023; Manso-Morato et al., 2025b).

Table 1
Density and water absorption of natural aggregates.

Aggregate	Siliceous 0-4 mm	Siliceous 4-12 mm	Siliceous 12-22 mm	Limestone 0-2 mm
Density (kg/dm^3)	2.62	2.63	2.60	2.66
Water absorption (% vol.)	0.12	0.32	0.55	0.10

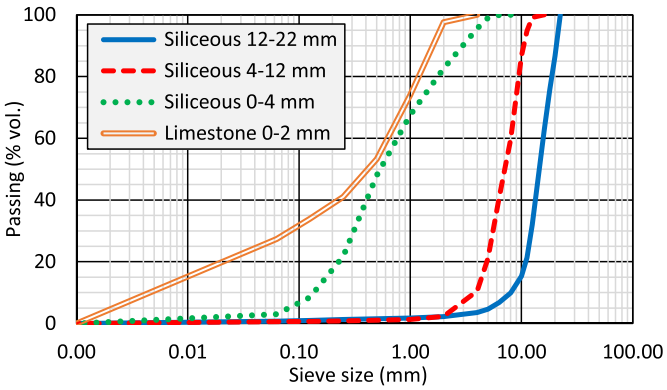

Fig. 1. Granulometric curves of aggregates.

2.2. Mix composition

A reference mix with 0% WTBW was designed following the guidelines established in Eurocode 2 (EC-2, 2010). Two design criteria were set to define the proportions of the raw materials, aiming to ensure the concrete mix had broad applicability. First, the fresh concrete was required to exhibit a slump between 100 and 150 mm, corresponding to slump class S3 according to EN 206 (Euronorm, 2026). Second, the target 28-day compressive strength was approximately 45 MPa. Based on these criteria, the cement content was set at 320 kg/m^3, with a plasticizer dosage of 1% by weight of cement and a water-to-cement ratio of 0.40. The aggregate proportions were determined by fitting the Fuller curve with a 0.5 exponent, as shown in Fig. 3. This ensured continuous particle size distribution and adequate fines content to achieve the desired workability (Revilla-Cuesta et al., 2023).

The mix containing 20% WTBW was designed by replacing 20% of the aggregate volume with this waste material. This substitution was carried out in such a way that the proportions between the different aggregate fractions remained unchanged. Moreover, following the design guidelines established by the authors' research group for the development of concrete with adequate workability containing up to 10% WTBW (Manso-Morato et al., 2025b), the plasticizer dosage was increased to 1.4% by weight of cement and the water-to-cement ratio to 0.52 upon the addition of 20% WTBW. This ensured that the concrete mix achieved adequate workability, thereby making it suitable for practical application in the construction and civil engineering sectors. The composition of both mixes is detailed in Table 3.

2.3. Experimental tests

First, the fresh performance of concrete was assessed by covering the slump, the air content, and the fresh density. All procedures were conducted following European standards (Euronorm, 2026) immediately after finishing mixing the concrete.

Fig. 2. WTBW: (a) overall material; (b) GFRP fibers; (c) GFRP microfibers; (d) balsa-wood particles; (e) polymeric particles.

Table 2
Proportion and size of WTBW components.

Component	GFRP fibers	GFRP microfibers	Polymeric particles	Balsa-wood particles	Small mixed particles
Proportion (% wt.)	66.8	13.8	8.3	6.3	4.8
Size (mm)	13.1	<10 mm	<10 mm	<10 mm	<1 mm

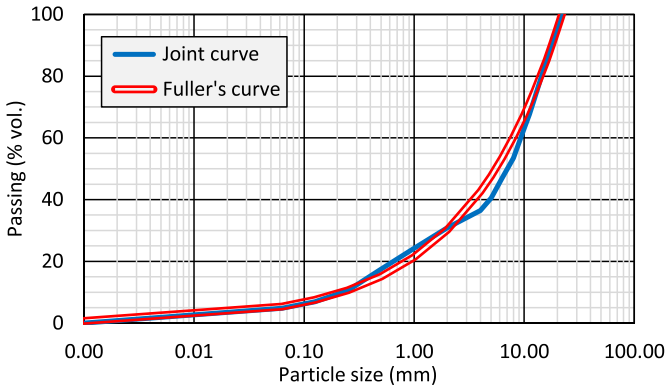

Fig. 3. Joint granulometric curve of aggregates in the concrete mixes.

Table 3
Comparative mix composition (kg).

Mix component	Cement	Water	Plasticizers	Aggregates 0-4 mm # 4-12 mm # 12-22 mm # 0-2 mm	WTBW
0% WTBW	320	128	3.20	385 # 555 # 780 # 280	0
20% WTBW	320	165	4.58	310 # 445 # 625 # 225	250

Another set of tests aimed to evaluate physical and mechanical performance of concrete. They were carried out at 28 days, following standardized European procedures (Euronorm, 2026), using three specimens per test and mix. Three different specimen types were used: Type I specimens were 10 cm cubic samples; Type II specimens were cylindrical, with a diameter of 10 cm and a height of 20 cm; and Type III specimens were prismatic, with a cross-section of 7.5 × 7.5 cm and 27.5-cm length. The evaluated properties included density, non-destructive properties (ultrasonic pulse velocity and rebound index), and mechanical properties, both strength-related (compressive, splitting tensile, and flexural strengths) and stiffness-related (modulus of elasticity and Poisson's ratio).

Finally, three tests were conducted to deepen the deformational behavior of concrete in the hardened state. They were also conducted at 28 days on three specimens per test and mix. Both load-deflection curves in bending, as well as longitudinal and transverse stress-strain curves in uniaxial compression, were evaluated. Loading was applied until the specimens were no longer load-bearing, following the loading rates specified in the relevant European standard procedures for compressive and flexural strength testing (Euronorm, 2026). The stress-strain curves under compression were obtained using Type II specimens. Load was measured with a load cell, and strains were recorded using strain gauges. The load-deflection curves were measured on Type III specimens, with load recorded through a load cell and deflection determined by the loading piston displacement of the testing press. Further details of the procedures can be found in previous research (Ortega-López et al., 2024).

Table 4 shows all the tests conducted, along with the type of specimen used and the standards applied in each case. The significance of the results of all these tests was determined statistically using a 95%-confidence one-way ANalysis Of VAriance (ANOVA).

The failure mechanisms of the mix containing 20% WTBW were analyzed at the meso-scale, *i.e.*, at the specimen level. The role of the GFRP microfibers in them was deepened by Scanning Electron Microscopy (SEM), performed with a microscope model JEOL JSM-6460LV. The fragments analyzed through SEM were extracted from specimens of the mix containing 20% WTBW that had been tested to flexural strength. Their average size was approximately 5 mm, and they were gold-coated prior to imaging.

Table 4
Experimental plan.

Test		Specimen type	Standard
Fresh state	Slump	Fresh sample	EN 12350-2
	Fresh density	Fresh sample	EN 12350-6
	Air content	Fresh sample	EN 12350-7
Hardened state: Physical and mechanical performance	Hardened density	Type I	EN 12390-7
	Ultrasonic pulse velocity	Type I	EN 12504-4
	Rebound index	Type II	EN 12504-2
	Compressive strength	Type II	EN 12390-3
	Splitting tensile strength	Type II	EN 12390-6
	Flexural strength	Type III	EN 12390-5
	Modulus of elasticity	Type II	EN 12390-13
	Poisson's ratio	Type II	EN 12390-13
Hardened state: Deformational behavior	Longitudinal stress-strain	Type II	EN 12390-3[a]
	Transverse stress-strain	Type II	EN 12390-3[a]
	Load-deflection	Type III	EN 12390-5[a]

[a] Standards adapted for the performance of the deformability tests.

2.4. Life cycle assessment (LCA): Framework and life cycle inventory (LCI)

The environmental impact of both concrete mixes was determined through an LCA conducted with SimaPro v9 software (Pré Sustainability, 2024). The ISO 14040/44 standard (Euronorm, 2026), the Ecoinvent v3 database (Ecoinvent Centre, 2024), and the CML-IA baseline methodology (CML, 2016) with a 100-year time horizon were used to perform it. In addition, a cradle-to-gate (A1-A3) approach was adopted with a consideration of excluding the past, *i.e.*, not considering the environmental impact of WTBW production. Thus, the recycling process for producing WTBW is considered to be limited to the wind energy sector and not to concrete production (Wei and Hadigheh, 2022). In this way, the LCA focuses on the environmental performance of concrete when this waste is incorporated, rather than on the environmental impacts of the various existing strategies for managing end-of-life wind turbine blades. The functional unit was 1 m^3 of freshly mixed concrete. All the aspects considered are common in this type of analyses relating to the effect of the use of sustainable raw materials on the environmental performance of concrete (Acosta-calderon et al., 2022; Frazão et al., 2022).

The LCI used for the LCA took the following considerations into account:

- First, conventional raw materials were modeled as items available in the Ecoinvent database (Ecoinvent Centre, 2024), always choosing the item most similar to actual conditions: cement with 6-20% limestone; tap water; plasticizer for concrete; and market for crushed gravel or limestone.
- Second, the packaging of the different raw materials was incorporated, considering that cement was supplied in 25 kg bags, plasticizers in 25-L bottles, and aggregates in 1 m^3 big-bags.
- Third, the environmental impact of transport was also included, which was assimilated as a diesel truck with a payload capacity of 16-32 metric tons (RER, EURO4). Transport distances of the raw materials corresponded to those between the point of acquisition of the raw material and the point of concrete production: 6.1 km for cement, 6.8 km for plasticizers, and 26.0 km for aggregates. Water did not require transport as it was taken from the local supply network.
- Finally, energy consumption during the mixing process was also incorporated to the LCA, being modeled as the medium-voltage electricity market in Spain. Concrete mixing always took 12 min.

The LCA carried out followed exactly the same criteria as those used in previous studies by the research group of the authors (Manso-Morato et al., 2025a, 2025b). Thus, the Abiotic Depletion Potential for fossil fuels (ADPf) and Global Warming Potential (GWP) indicators were studied, as they are the most relevant in concrete and, in turn, the most influenced by the use of sustainable raw materials (Manso-Morato et al., 2025a).

3. Results and discussion

3.1. Fresh behavior

The results of the fresh measurements of both mixtures are detailed in Table 5. The addition of 20% WTBW led to a deterioration in the fresh behavior of concrete, although the values obtained in all cases remained within suitable ranges for the proper use of this construction material (Metha and Monteiro, 2014).

Table 5
Results of fresh properties.

Property	0% WTBW	20% WTBW
Slump (mm)	147 ± 8	90 ± 4
Fresh density (kg/dm^3)	2.42 ± 0.02	2.17 ± 0.01
Air content (% vol.)	2.2 ± 0.1	4.5 ± 0.1

The addition of 20% WTBW led to a slump reduction of approximately 39%, the mixture containing 20% WTBW being classified as slump class S2 (slump between 50 and 90 mm according to EN 206 (Euronorm, 2026)). The high proportion of GFRP fibers and microfibers present in this waste formed a three-dimensional network that limited the cement paste's ability to successfully drag the aggregate particles, as found for other fiber types (Biswas et al., 2021). Additionally, the waste components exhibited a higher specific surface area than the aggregates they replaced, which may have impaired their lubrication following available literature (Güneyisi et al., 2019). Polymeric and balsa wood particles also contributed to this behavior due to their angular shape caused by crushing, which made their mobilization by the cement paste difficult, as literature reports for other plastic aggregates (Coviello et al., 2024).

Air content doubled following the addition of 20% WTBW. Research on conventional fibers (Biswas et al., 2021) lead to deduction that the three-dimensional network formed by the GFRP fibers and microfibers also caused a greater amount of air to be entrapped within the fresh concrete mass. While it is thought that polymeric particles did not significantly affect this property, balsa wood particles did. Balsa wood is highly porous and has a very low density (Jang and Kang, 2022), so these particles may have acted as pores regarding this test.

Finally, the fresh density decreased by 0.25 kg/dm^3 with the addition of 20% WTBW, due to three reasons supported by the conclusions of other similar research. First, the lower density of the blade waste compared to the aggregates it replaced (Coviello et al., 2024). Second, the increased porosity induced by this waste, resulting from the aforementioned fiber network and the balsa wood porosity (Revilla-Cuesta et al., 2024b). And third, the increased porosity caused by the rise in the water-to-cement ratio from 0.40 to 0.52 when this residue was added in order to maintain proper workability (Guo et al., 2025).

3.2. Physical and mechanical performance

The results of the physical and mechanical properties of the mixtures at 28 days are presented in Table 6. From an overall perspective, the values of all properties decreased as a consequence of the incorporation of WTBW, although there were some exceptions that are worth highlighting.

Firstly, hardened density decreased by approximately 13%, in a manner similar to that observed in the fresh state. After analyzing the similar performance in available research (Revilla-Cuesta et al., 2024b; Vieira et al., 2016), this reduction was attributed to the lower real density of WTBW than that of natural aggregate, further accentuated by the high porosity of balsa wood, whose particles present in this residue acted as air-filled voids with respect to this property. Additionally, the increase in matrix porosity due to the higher water-to-cement ratio also contributed to this behavior.

With respect to mechanical strengths, both compressive and splitting tensile ones experienced a significant reduction. Compressive strength decreased by 63%, mainly due to the higher water-to-cement ratio, but

Table 6
Results of 28-day hardened properties.

Property	0% WTBW	20% WTBW
Hardened density (kg/dm^3)	2.43 ± 0.01	2.12 ± 0.01
Ultrasonic pulse velocity (km/s)	4.88 ± 0.09	4.13 ± 0.07
Rebound index (−)	37.3 ± 1.2	26.0 ± 2.0
Compressive strength (MPa)	47.2 ± 3.4	17.6 ± 3.0
Splitting tensile strength (MPa)	4.19 ± 0.22	3.09 ± 0.32
Flexural strength (MPa)	5.59 ± 0.52	5.59 ± 0.23
Modulus of elasticity (GPa)	45.3 ± 0.9	13.2 ± 1.3
Poisson's ratio (−)	0.167 ± 0.015	0.109 ± 0.016

also because of the existence of balsa wood and polymeric particles in this residue, for which previous research (Manso-Morato et al., 2025b) suggests that they could act as weak points from which failure of the specimens could initiate and propagate. In addition, their ITZ with the cementitious matrix may have exhibited weakness and caused slippage, according to previous analyses of mixtures containing up to 10% WTBW (Manso-Morato et al., 2025c). The GFRP fibers and microfibers did not contribute effectively in this regard, since the confinement they provided to concrete under failure loads was not effective in strength terms. Nevertheless, their ITZ were almost certainly characterized by high density, compactness, and adhesion, as documented in previous concrete mixes containing 10% WTBW (Manso-Morato et al., 2025c). A reduction in splitting tensile strength was also observed, as these weak particles exhibited lower bonding with the cementitious matrix compared to natural aggregate, thereby leading to a reduced failure stress according to available literature (Revilla-Cuesta et al., 2024a). However, the decrease in this strength was limited to 26%, which can be attributed to the stitching effect of GFRP fibers and microfibers, as also yielded on research on such kind of fibers (Xu et al., 2022). The real stitching effect of the GFRP fibers and microfibers was observed in flexural strength, which remained constant at 5.59 MPa despite the incorporation of WTBW. In spite of the reduction in the quality of the cementitious matrix due to the aforementioned factors, this property remained unchanged thanks to the effective stitching provided by the fibers and microfibers in the tensile zone of the specimen, favored by the quality of the ITZ they generated according to previous studies (Manso-Morato et al., 2025c).

The effect of WTBW on the stiffness properties of concrete in the elastic regime also varied depending on the direction considered. On the one hand, WTBW made the concrete more deformable in the longitudinal loading direction, with a reduction of the modulus of elasticity of up to 71%. From the conclusions available in the scientific literature, this behavior was attributed to the lower quality of the cementitious matrix due to the increased water-to-cement ratio (Vieira et al., 2016) and the presence of weak and deformable polymeric and balsa wood particles (Borrega and Gibson, 2015; Coviello et al., 2024). On the other hand, the incorporation of the blade waste increased the elastic stiffness in the transverse direction to the load, as evidenced by a 35% reduction in Poisson's ratio. In the elastic regime, unlike under failure conditions, GFRP fibers and microfibers effectively confined the concrete, limiting its bulging and, consequently, its transverse deformation, as literature also shows (Ortega-López et al., 2024).

Finally, the two non-destructive properties evaluated, ultrasonic pulse velocity and rebound index, decreased by 15% and 30%, respectively, when 20% of WTBW was incorporated. Ultrasonic pulse velocity is related to porosity, density, and elastic stiffness of the cementitious matrix (Jones, 1963). With the addition of WTBW, porosity increased, with balsa wood particles acting as air-filled voids, while both density and elastic stiffness decreased significantly, resulting in a reduction of this velocity. However, the decrease was not very pronounced, since the GFRP fibers and microfibers acted as conductors of the ultrasonic wave, thereby limiting this reduction, as the ultrasonic pulse velocity of GFRP is approximately 2.5 km/s (Abd El-Malak, 1997). The deterioration in the cementitious matrix quality due to the incorporation of WTBW was more clearly reflected in the rebound index. The water content increase, together with the existence of polymeric and balsa wood particles of low hardness, were the main factors responsible for this outcome, as supported by other scientific research (Bawa et al., 2023).

3.3. Deformational performance

3.3.1. Longitudinal stress-strain curve under compression

Fig. 4 shows the longitudinal stress-strain curves under compression for the mixtures containing 0% and 20% WTBW. From a general analysis, the curve of the mix incorporating 20% WTBW revealed a higher curvature and a more horizontal trend, thus exhibiting greater ductility and deformation capacity (Liu et al., 2025b).

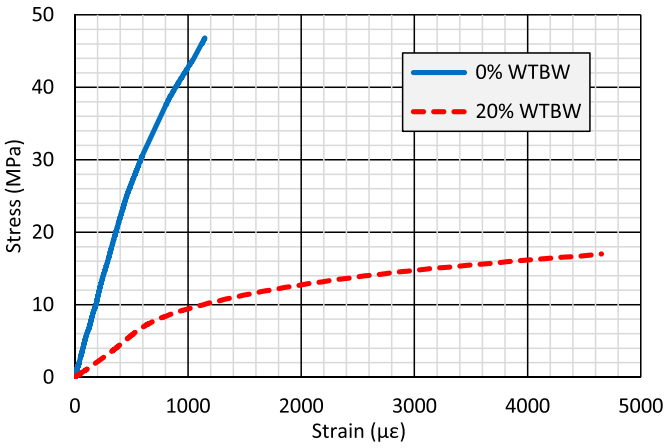

Fig. 4. 28-day longitudinal stress-strain curves under compression.

This initial observation was supported by the values of peak and fracture strains, which are detailed in Table 7. Both strains increased when 20% WTBW was added to concrete, being approximately quadrupled (4653 με versus 1148 με). Therefore, plastic strains followed a trend similar to that of the elastic modulus. Based on scientific literature (Borrega and Gibson, 2015; Revilla-Cuesta et al., 2024a), such performance could be due to the higher deformability of the cementitious matrix when adding WTBW caused by the increased water-to-cement ratio and the presence of balsa wood and polymer particles in the residue, both of which are more flexible than natural aggregate. Moreover, the GFRP fibers and microfibers could also have exerted a confinement effect on concrete, which may have also contributed to greater longitudinal deformation prior to failure. However, it should also be noted that the concrete exhibited no post-peak load-bearing capacity when 20% WTBW was added, as the peak and fracture strains coincided. It is believed that, despite the potentially beneficial effect of the GFRP microfibers and fibers in this regard, the weakness of the cementitious matrix, evidenced by the significant reduction in compressive strength, led the concrete mix to an inability to sustain load after failure. In terms of the area enclosed under the curve, that is, absorbed energy (Table 7), the addition of 20% WTBW nearly doubled this value (an increase of approximately 82%). It is therefore clear that the higher elastic and plastic deformability of concrete resulting from the incorporation of this amount of waste compensated, in energy terms, for the marked decrease in compressive strength.

3.3.2. Transverse stress-strain curve under compression

Fig. 5 shows the transverse stress-strain curves in compression, while Table 8 summarizes the main transverse stress-strain properties. As in the longitudinal direction, the addition of WTBW yielded a curve with greater curvature and a more horizontal shape, indicating an increase in the ductility of concrete (Liu et al., 2025b).

When assessing the concrete's plastic deformability, it was noted that both the peak and fracture strain increased with the addition of WTBW. Thus, the peak strain was approximately ten times higher, while the fracture strain increased by around 50%. The inclusion of WTBW notably enhanced the energy-absorption capacity of concrete up to failure in the transverse direction, probably because of the confinement

Table 7
28-day longitudinal stress-strain properties under compression.

Property	0% WTBW	20% WTBW
Peak strain (με)	1148 ± 61	4653 ± 157
Fracture strain (με)	1148 ± 61	4653 ± 157
Absorbed energy (MJ/m^3)	0.0312 ± 0.0005	0.0567 ± 0.0007

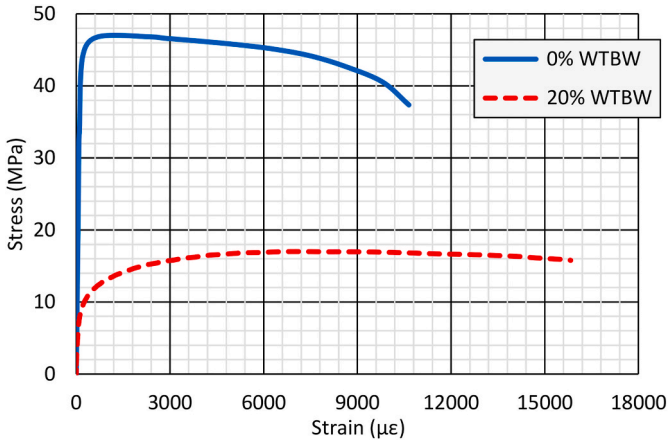

Fig. 5. 28-day transverse stress-strain curves under compression.

Table 8
28-day transverse stress-strain properties in compression.

Property	0% WTBW	20% WTBW
Peak strain (με)	692 ± 23	7032 ± 244
Fracture strain (με)	10649 ± 294	15831 ± 327
Absorbed energy (MJ/m^3)	0.4720 ± 0.0012	0.2535 ± 0.0009

effect exerted by the GFRP fibers and microfibers properly oriented within the test specimens. However, although WTBW was indeed capable of providing load-bearing capacity in the transverse direction to a compression load, the post-peak behavior was not so significantly affected by this waste. In fact, the strain increment from the peak to the fracture point slightly decreased with the addition of this residue. This phenomenon could be a consequence of the cementitious matrix weakening caused by the high flexibility of the polymer particles and balsa wood present in the waste, as reflected by the literature (Borrega and Gibson, 2015; Islam et al., 2022), as well as the necessary adjustment in the water content to maintain adequate workability in the fresh state when adding it. As previously discussed, such weakening also led to a reduction in compressive strength. Therefore, the decrease in compressive strength and in the strain increment from failure to fracture caused the total absorbed energy in the transverse direction to be reduced by approximately 46% when 20% WTBW was incorporated into concrete.

3.3.3. Load-deflection curve under bending

Fig. 6 shows the load-deflection curves under bending for the two concrete mixes studied, while Table 9 summarizes the most relevant properties derived from them. In this case, a clear distinction could be made between the behavior before and after failure, *i.e.*, relative to the maximum load point (flexural strength):

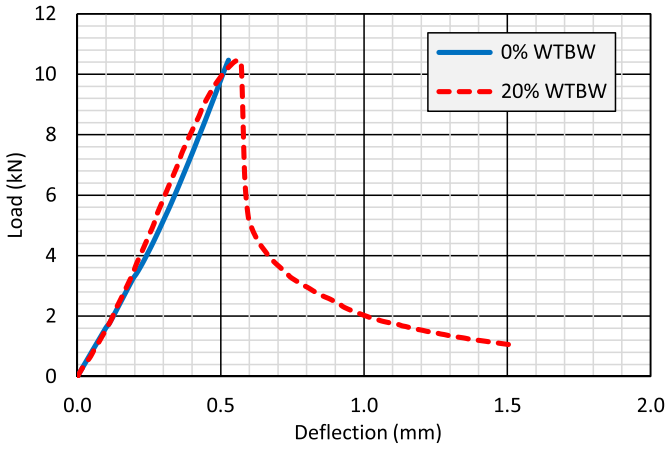

Fig. 6. 28-day load-deflection curves under bending.

- The addition of 20% WTBW did not significantly affect the pre-failure behavior of concrete. Both the reference mix and the one containing 20% waste exhibited practically the same compliance (stiffness expressed as the inverse slope of the linear segment before failure) and peak deflection, with values around 0.044 mm/kN and 0.54 mm, respectively. This observation was consistent with the results obtained for flexural strength, the use of WTBW not affecting it. The GFRP fibers and microfibers proved highly effective in stitching the cementitious matrix, limiting deformability before failure despite the matrix weakening caused by the increased water-to-cement ratio and the presence of weak particles in the residue, as reported in similar studies (Revilla-Cuesta et al., 2024a; Islam et al., 2022).
- The post-failure behavior of concrete was notably impacted by the addition of 20% WTBW. The reference mixture exhibited a brittle failure, with the peak and fracture deflections being identical. In contrast, the mix containing WTBW showed a clear load-bearing capacity after failure, being able to sustain load at deflection levels nearly three times higher than the peak deflection. The GFRP fibers and microfibers continued to act effectively after cracking, bridging the fractured cementitious matrix in the tension zone and thereby maintaining structural integrity beyond the failure point, as other research on concrete containing GFRP fibers from end-of-life wind turbine blades of different nature has also shown (Yazdanbakhsh et al., 2018; Xu et al., 2022).

As a result of preserving pre-failure behavior and enhancing post-failure load-bearing capacity by adding 20% WTBW, the absorbed energy under bending of this concrete mix increased by 114% compared to the reference concrete mix. This was the type of mechanical solicitation in which the improvement caused by the addition of 20% WTBW was most noticeable.

3.4. Analysis of statistical significance

The significance of the effect of WTBW addition on the concrete's behavior was evaluated by means of a one-way ANalysis Of VAriance (ANOVA), considering the factor "WTBW content". This analysis was conducted at a 95% confidence level (*i.e.*, a 5% significance level) and included all individual experimental results obtained from all the tested specimens. Accordingly, a *p*-value lower than 0.05 means that the waste content had a statistically significant effect on concrete's behavior. This type of analysis is common in research related to concrete science (Cantero et al., 2018).

The results, presented in Table 10, show that all the concrete properties were significantly affected by the incorporation of 20% WTBW, except for the flexural strength and the pre-failure deformational properties in bending (*i.e.*, compliance and peak deflection). Hence, the addition of 20% WTBW on the concrete properties analyzed is significant and must be accounted for in both the improvement and deterioration it causes.

Table 9
28-day load-deflection properties under bending.

Property	0% WTBW	20% WTBW
Compliance (mm/kN)	0.0438 ± 0.0012	0.0451 ± 0.0009
Peak deflection (mm)	0.527 ± 0.026	0.559 ± 0.019
Fracture deflection (mm)	0.527 ± 0.026	1.511 ± 0.031
Absorbed energy (J)	2.503 ± 0.074	5.344 ± 0.093

Table 10
ANOVA results.

Property		*P*-value
Fresh properties	Slump	0.0004
	Fresh density	0.0000
	Air content	0.0000
Mechanical properties	Hardened density	0.0000
	Ultrasonic pulse velocity	0.0003
	Rebound index	0.0092
	Compressive strength	0.0003
	Splitting tensile strength	0.0339
	Flexural strength	0.9949
	Modulus of elasticity	0.0000
	Poisson coefficient	0.0275
Longitudinal stress-strain properties in compression	Peak strain	0.0000
	Fracture strain	0.0000
	Absorbed energy	0.0000
Transverse stress-strain properties in compression	Peak strain	0.0000
	Fracture strain	0.0000
	Absorbed energy	0.0000
Load-deflection properties in bending	Compliance	0.2077
	Peak deflection	0.1603
	Fracture deflection	0.0000
	Absorbed energy	0.0000

3.5. Failure modes and mechanisms

In addition to the mechanical and deformation-related properties, this research also included an analysis of the failure modes and mechanisms of the tested specimens. These failure modes are illustrated in Fig. 7 (under compression) and Fig. 8 (under bending) and are further complemented by a microstructural analysis of the failure mechanisms performed using SEM, presented in Fig. 9.

Under compressive loading, the reference mixture exhibited a sudden and brittle failure, as shown in Fig. 7a. A clearly defined crack that appeared at the failure point can be observed, along with local surface spalling resulting from stress concentration in that region. In contrast, the mixture containing 20% WTBW exhibited a much more ductile and less pronounced failure mode. As illustrated in Fig. 7b, cracks appeared in the specimens of this concrete mix when failure, but they were characterized by a significantly smaller crack width and no visible damage to the specimen's skin. This failure mode was consistent with the observed increase in concrete deformability prior to failure due to a confinement effect of GFRP fibers and microfibers, mainly in the longitudinal direction relative to the compression load, thereby increasing the absorbed energy up to that point. Once this cracking occurred, and therefore failure, the GFRP fibers and microfibers were unable to provide load-bearing capacity because of the cementitious matrix deterioration caused by 20% WTBW incorporation, which promoted fiber debonding in accordance with similar research (Jiang et al., 2025). Nevertheless, it is evident that the GFRP fibers and microfibers effectively fulfilled their role, stitching the cementitious matrix and limiting crack propagation at the onset of compressive failure.

The GFRP fibers' bridging effect at the failure point was much more evident in the specimens tested under bending, as shown in Fig. 8. Under this type of stress, the cracks that appeared in the concrete mixture containing 20% WTBW exhibited a wider opening but were effectively stitched by the GFRP fibers contained in this waste. These GFRP fibers were appropriately oriented perpendicular to the casting direction, forming a three-dimensional reinforcement network. This configuration of the GFRP fibers within the concrete allowed the flexural strength to remain unchanged thanks to their bridging effect, despite the addition of 20% WTBW, since this property mainly depends on the behavior of the tensile zone of the specimen (Yazdanbakhsh et al., 2018). Moreover, the GFRP fibers helped maintain the integrity of the tested specimens after failure, enabling them to sustain load beyond the peak point and providing concrete with load-bearing capacity, as also found in other research (Xu et al., 2022). However, this meso-scale analysis did not

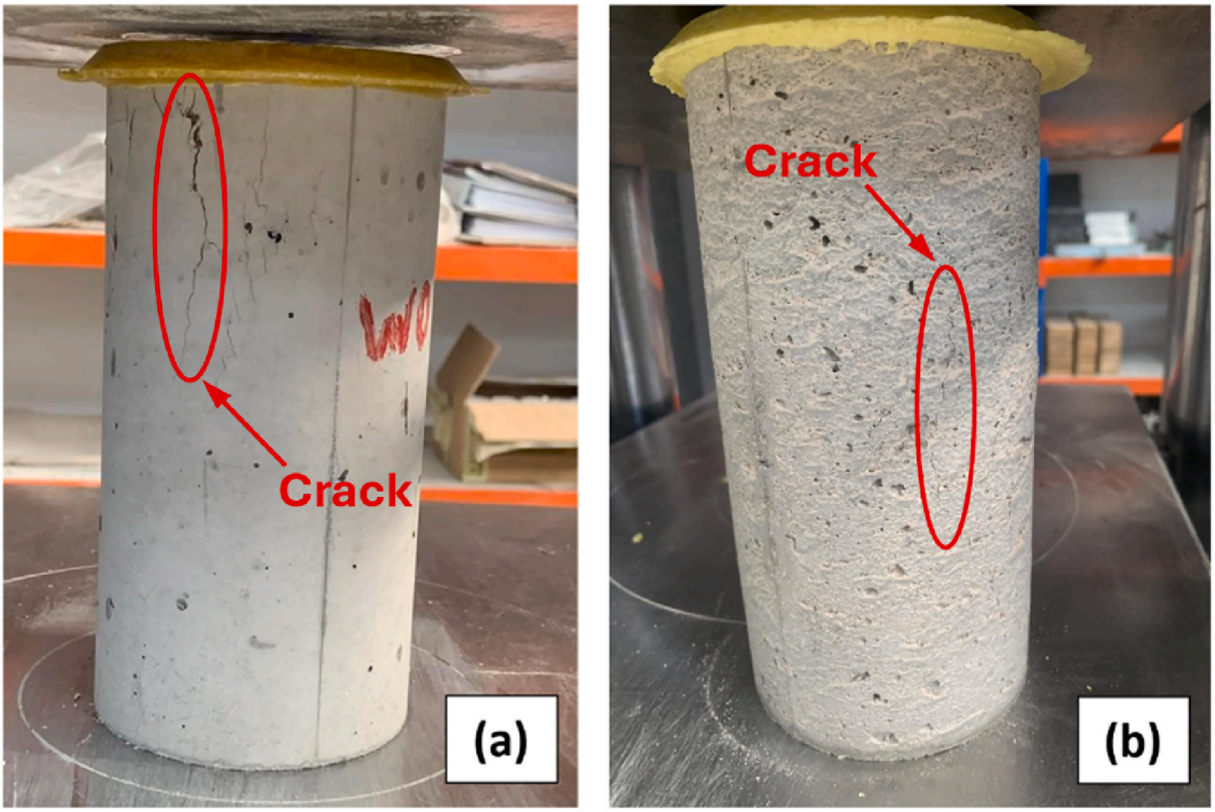

Fig. 7. Failure mode under compression: (a) 0% WTBW; (b) 20% WTBW.

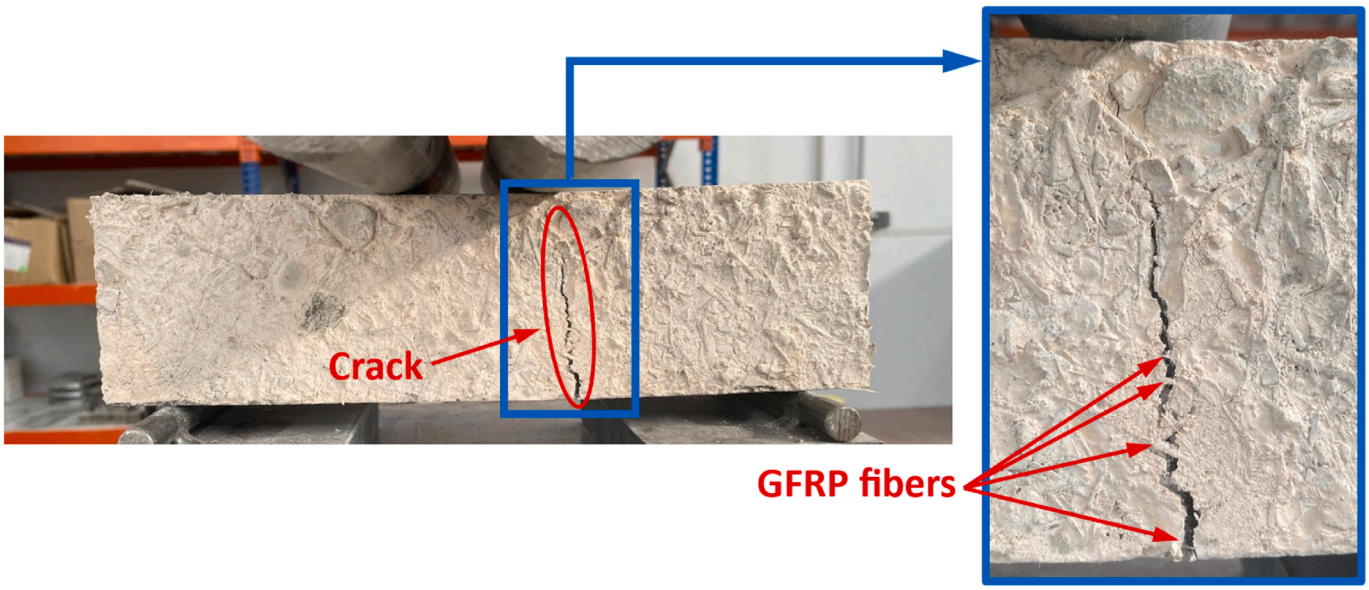

Fig. 8. Failure mode under bending of concrete with 20% WTBW. View from the concreting face of the specimen.

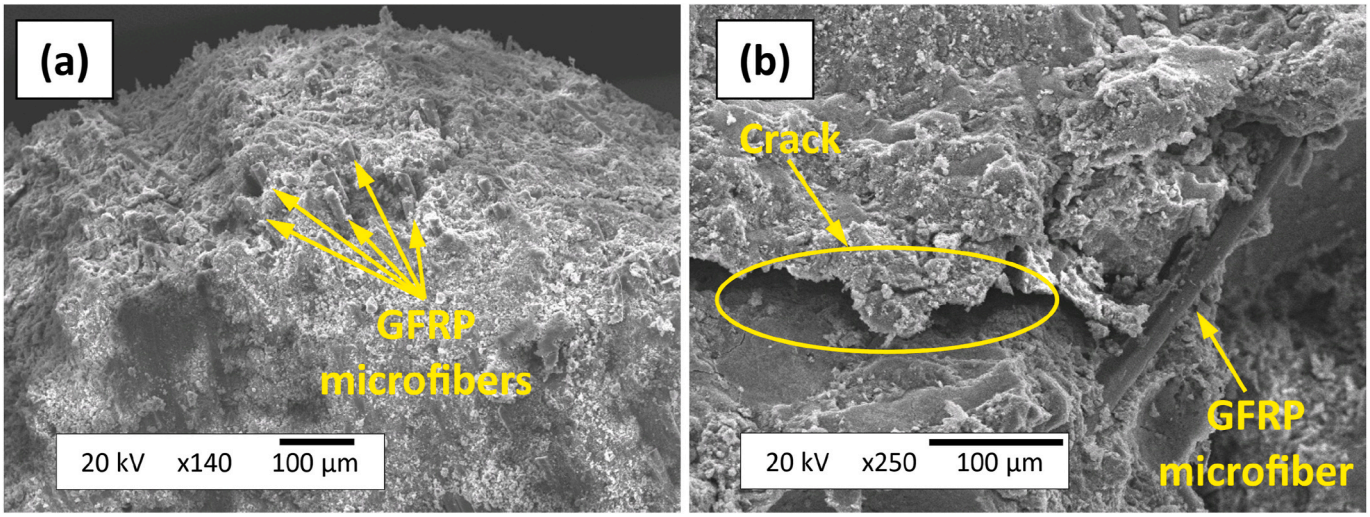

Fig. 9. SEM analysis of GFRP microfibers: (a) orientation; (b) matrix stitching.

allow a detailed evaluation of the role of the GFRP microfibers, which was carried out in a finer-scale examination.

The role of the GFRP microfibers was evaluated through a SEM analysis performed on fragments taken from the interior of specimens of the concrete mix containing 20% WTBW tested to flexural strength. The most relevant images obtained are shown in Fig. 9, which highlight two key aspects. First, Fig. 9a shows that all GFRP microfibers exhibited a parallel orientation, which, considering the direction from which the analyzed fragment was obtained, was perpendicular to the casting direction. Second, a microcrack can be observed in Fig. 9b, whose propagation was restrained by the stitching action of a GFRP microfiber visible on the right-hand side of the image. In general, the behavior of the GFRP microfibers was found to be analogous to that of the larger GFRP fibers observed in the meso-scale analysis of the specimens subjected to bending. Therefore, the GFRP microfibers were properly oriented after casting and effectively stitched the microcracks within the cementitious matrix, thereby contributing both to the retention of flexural strength after WTBW addition and to the post-failure load-bearing capacity of the concrete, as found for other plastic fibers of larger size in other studies (Xu et al., 2022; Coviello et al., 2024). Thus, the complete gradation of sizes of GFRP fibers and microfibers contained in the WTBW was beneficial in this regard.

3.6. *Life cycle analysis (LCA)*

The results obtained from the LCA are shown in Fig. 10. First, the total values obtained are depicted, followed by the results per unit of strength or absorbed energy.

The addition of 20% WTBW reduced the environmental impact per cubic meter of freshly mixed concrete by 5.7% in terms of GWP and 6.5% in terms of ADPf (Fig. 10a). This decrease was due to the replacement of natural aggregates with a waste, in this case WTBW, which has zero associated environmental burdens (Frazão et al., 2022). In addition, volumetric adjustments due to the increase in water and plasticizer content when incorporating WTBW implied a decrease in the cement content per concrete cubic meter. This is the raw material of concrete whose production generates the greatest environmental impact (Acosta-calderon et al., 2022). These results were consistent with those obtained in the case of blade repurposing, where some estimates indicate that approximately 342 $kgCO_2eq$ would be reduced for every ton of

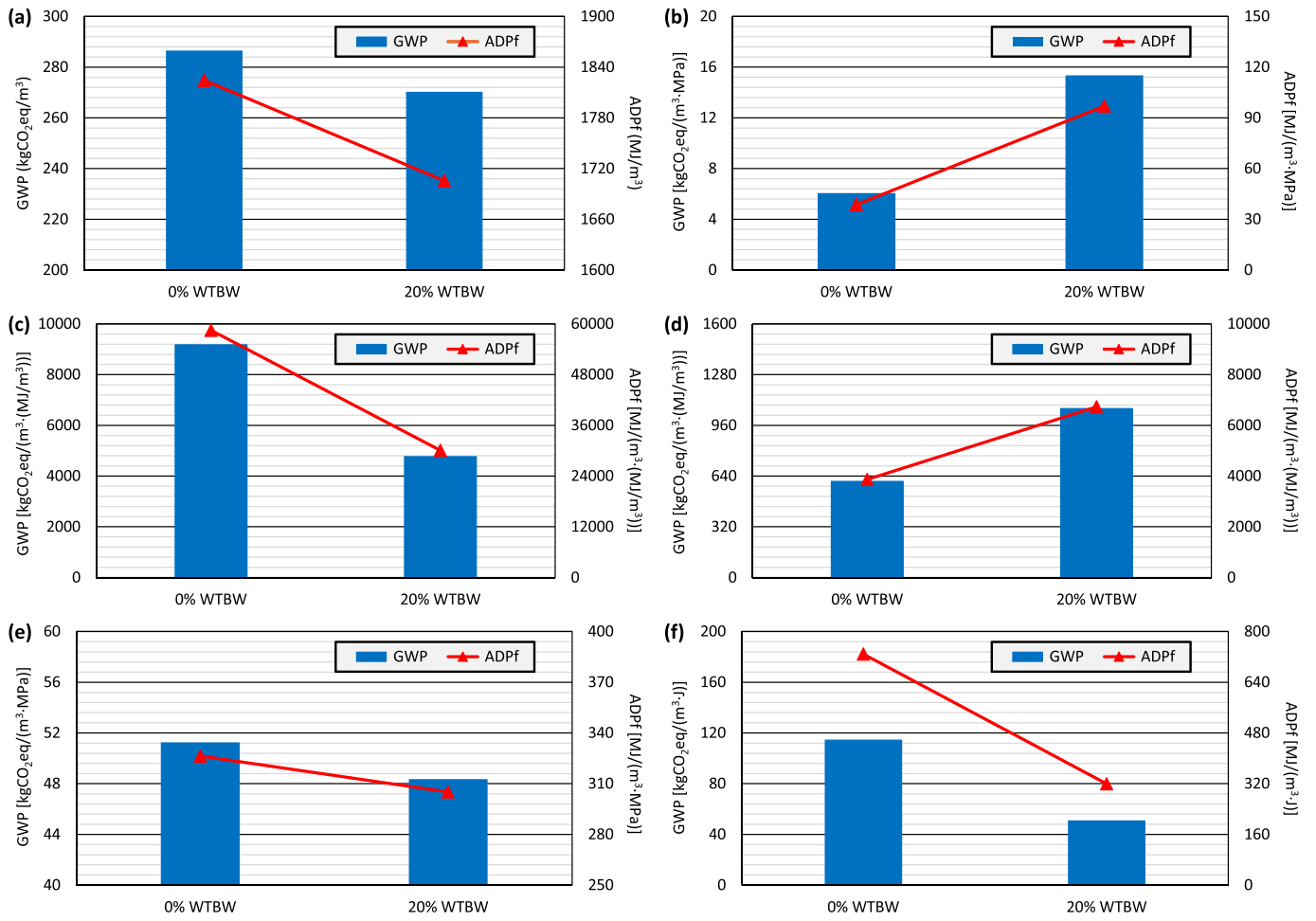

Fig. 10. LCA results: (a) total values; (b) per unit of compressive strength; (c) per unit of absorbed energy in compression in the longitudinal direction; (d) per unit of absorbed energy under compression in the transverse direction; (e) per unit of flexural strength; (f) per unit of absorbed energy under bending.

dismantled wind turbine blades effectively repurposed (Nagle et al., 2022). The most beneficial option would be to repurpose wind turbine blades as a substitute for steel components (Henao et al., 2024). In fact, the optimal and more feasible repurposing rate is established at around 20% of the dismantled wind turbine blades (Nagle et al., 2022), exactly the same amount of WTBW that has been added to concrete in this study.

When analyzing the environmental impact per unit of compressive strength (Fig. 10b) and per unit of flexural strength (Fig. 10e), the results are opposite. Under compression stresses, the addition of 20% WTBW increased the environmental impact by around 150%, both in terms of GWP and ADPf. This was due to the relevant decrease in compressive strength caused by WTBW due to cement matrix weakening by the deformable particles present in this waste and the increased water-to-cement ratio, with GFRP fibers and microfibers not being effective in increasing concrete strength under these loading conditions. On the contrary, these GFRP fibers and microfibers were effective under bending stresses, as also revealed in the scientific literature (Yazdanbakhsh et al., 2018; Xu et al., 2022). Therefore, the addition of WTBW caused the flexural strength to remain constant when WTBW was added, and in turn, the environmental impact under this type of stress decreased by around 6% per MPa of strength. The environmental impact per unit of absorbed energy followed the same trends, although the environmental impact per unit of absorbed energy under compression in the longitudinal direction (Fig. 10c) did decrease when adding WTBW due to the proper confinement of concrete in this direction thanks to the GFRP fibers and microfibers contained in this waste.

3.7. Overall analysis

To conclude the analysis of results, Fig. 11 shows a radar chart with the properties of the mixes under compression and bending. The values were normalized by taking a value of 1 for the best value of each property, the others being determined by direct proportionality (mechanical properties) or inverse proportionality (environmental

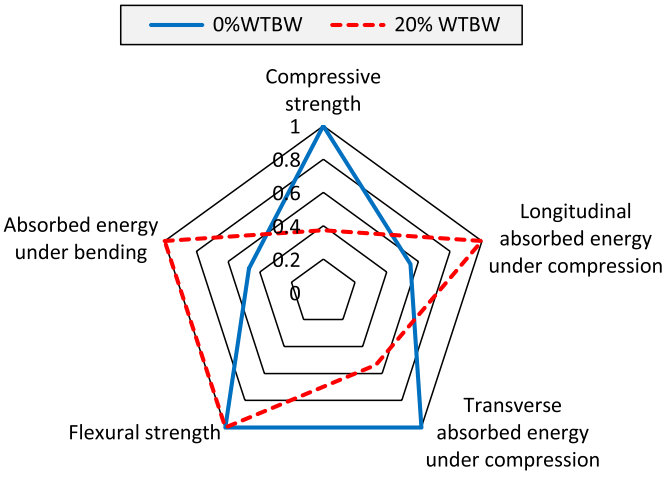

Fig. 11. Overview of concrete properties (radar chart identical for mechanical properties and environmental indicators).

indicators). The resulting normalized values were the same for the mechanical properties and environmental indicators (GWP and ADPf) of each mixture, the radar chart being therefore identical for both. From this representation, it is easy to see that in terms of strength, the mixture with 0% WTBW performed best, with the highest values for both strengths and the minimum environmental impacts per unit of them. However, in deformational terms, the mixture with 20% WTBW presented greater advantages, mainly with respect to energy absorption in bending and in the direction parallel to a compression load. In addition, it should be noted that the flexural strength of the mixture with 20% WTBW was exactly the same as that of the reference concrete mix. Therefore, the addition of 20% WTBW could be recommended in elements in which mechanical requirements are not high and bending stresses are predominant, such as pavements (Chen et al., 2023), lean concrete (Kumar, 2016), or continuous pipes supported on the ground (Kallenbacn et al., 2006).

4. Conclusions

The search for effective solutions for the recycling and valorization of decommissioned wind turbine blades has become an urgent necessity. One potential approach involves crushing the blades without selective separation, yielding a by-product that can be used as a concrete component. In this study, the fresh, mechanical, deformational, and sustainability behavior of concrete containing 20% Wind Turbine Blade Waste (WTBW) was analyzed. From this study, the following conclusions can be drawn:

- The fresh-state behavior was slightly impaired by the addition of 20% WTBW. However, the concrete still achieved a slump class S2 according to EN 206 (Euronorm, 2026). Thus, in principle, the mixture containing this amount of waste presented adequate workability for placement using conventional vibration.
- The mechanical properties of concrete in general were adversely affected by the weak balsa wood and polymer particles in the WTBW, as well as by the required adjustment of water and plasticizer contents. Nevertheless, the flexural strength remained unchanged despite the addition of 20% WTBW, owing to the stitching effect of fibers and microfibers from Glass Fiber-Reinforced Polymer (GFRP).
- The energy absorption capacity of concrete was also enhanced, probably due to the stitching action of the GFRP fibers and microfibers. These fibers confined concrete in the longitudinal direction under compressive loading and provided a significant post-failure load-bearing capacity in bending. The absorbed energy under flexural loading was almost doubled when incorporating 20% WTBW.
- The failure modes of concrete under both compression and bending became more ductile with the incorporation of 20% WTBW, with cracks showing smaller widths and no surface spalling of the specimens. This improvement was attributed to the proper orientation of the GFRP fibers, whose major axis was perpendicular to the casting direction, forming a three-dimensional reinforcement. Scanning electron microscopy confirmed that the GFRP microfibers exhibited the same behavior.
- Abiotic depletion potential for fossil fuels and global warming potential, determined through a cradle-to-gate life cycle assessment, were reduced by approximately 6% when 20% WTBW was added. Furthermore, the environmental impact per unit of strength or absorbed energy under bending also decreased. These improvements may be due to the reduction in the content of cement and natural aggregates by adding WTBW, while preserving the bending performance.

All the above-mentioned effects were statistically significant following an analysis of variance, which supports the potential use of concrete containing 20% WTBW in applications with soft mechanical requirements and in which bending stresses are predominant. Non-structural applications, such as pavements, lean concrete, urban furniture, and continuous pipes supported on the ground, among others, could, in theory, be a feasible option. However, given the deduced technical feasibility of adding 20% WTBW to concrete when used for the described applications, future research should evaluate its durability performance and porosity results, including analyses through mercury intrusion porosimetry, for a complete assessment of the implications of producing concrete with such a high amount of WTBW. An in-depth assessment of the interfacial transition zones of the various components of WTBW, as well as X-ray diffraction and energy-dispersive spectroscopy analyses, would also be necessary to clearly understand the role of each WTBW component when this waste is incorporated in such large quantities. Producing concrete mixes with a 20% WTBW but without modifying the water content would allow for a more in-depth examination of the impact of adjusting the water-to-cement ratio. Finally, leaching toxicity tests would also be necessary for a complete environmental characterization of concrete with 20% WTBW.

CRediT authorship contribution statement

Víctor Revilla-Cuesta: Conceptualization, Data curation, Formal analysis, Investigation, Methodology, Software, Writing – original draft. **Javier Manso-Morato:** Conceptualization, Investigation, Software, Validation, Visualization, Writing – review & editing. **Ana B. Espinosa:** Data curation, Formal analysis, Supervision, Validation, Visualization. **Marta Skaf:** Funding acquisition, Project administration, Resources, Supervision, Validation, Visualization, Writing – review & editing.

Declaration of competing interest

The authors declare that they have no known competing financial interests or personal relationships that could have appeared to influence the work reported in this paper.

Acknowledgements

This research work was supported by grant TED2021-129715B-I00 funded by MICIU/AEI/10.13039/501100011033 and by European Union NextGenerationEU/PRTR; grant PID2023-146642OB-I00 funded by MICIU/AEI/10.13039/501100011033 and by ERDF/EU; grant FPU21/04364 funded by MICIU; grants UIC-231 and BU033P23 funded by the Junta de Castilla y León (Regional Government) and ERDF/EU; and grant SUCONS, Y135.GI funded by the University of Burgos.

Data availability

Data will be made available on request.

References

Abd El-Malak, N.A., 1997. Ultrasonic properties of composites (polymer-fibre glass). Bull. Mater. Sci. 20 (7), 981–990. https://doi.org/10.1007/BF02744886.

Acosta-calderon, S., Gordillo-silva, P., García-troncoso, N., Bompa, D.V., Flores-rada, J., 2022. Comparative evaluation of sisal and polypropylene fiber reinforced concrete properties. Fibers 10 (4), 31. https://doi.org/10.3390/fib10040031.

Asociación Empresarial Eólica (AEE), 2024. Record Year for Wind Power in 2023.

Bawa, S., Alam, P., Saini, S., 2023. Evaluation of performance of hybrid fiber-reinforced self-compacting concrete using non-destructive testing techniques. Innov. Infrastruct. Solut. 8 (4), 126. https://doi.org/10.1007/s41062-023-01092-y.

Biswas, R.K., Bin Ahmed, F., Haque, M.E., Provasha, A.A., Hasan, Z., Hayat, F., Sen, D., 2021. Effects of steel fiber percentage and aspect ratios on fresh and Harden properties of ultra-high performance fiber reinforced concrete. Appl. Mech. 2 (3), 501–515. https://doi.org/10.3390/applmech2030028.

Borrega, M., Gibson, L.J., 2015. Mechanics of balsa (Ochroma pyramidale) wood. Mech. Mater. 84, 75–90. https://doi.org/10.1016/j.mechmat.2015.01.014.

Cantero, B., Sáez del Bosque, I.F., Matías, A., Medina, C., 2018. Statistically significant effects of mixed recycled aggregate on the physical-mechanical properties of structural concretes. Constr. Build. Mater. 185, 93–101. https://doi.org/10.1016/j.conbuildmat.2018.07.060.

Chen, L., Chen, Z., Xie, Z., Wei, L., Hua, J., Huang, L., Yap, P.S., 2023. Recent developments on natural fiber concrete: a review of properties, sustainability,

applications, barriers, and opportunities. Dev. Built Environ. 16, 100255. https://doi.org/10.1016/j.dibe.2023.100255.
CML - Department of Industrial Ecology, CML-IA Characterisation Factors, 2016.
Coviello, C.G., La Scala, A., Sabbà, M.F., Carnimeo, L., 2024. On the cementitious mixtures reinforced with waste polyethylene terephthalate. Materials 17 (21), 5351. https://doi.org/10.3390/ma17215351.
DarvishaliNezhad, A., Mousavinejad, S.H.G., Gholizad, A., 2026. Optimization of sustainability in GFRP-reinforced concrete: experimental, numerical and environmental assessment. J. Build. Pathol. Rehabilit. 11 (1), 9. https://doi.org/10.1007/s41024-025-00683-9.
Das Karmakar, S., Chattopadhyay, H., 2025. A comprehensive look into the sustainability of wind power. Renew. Sustain. Energy Rev. 217, 115694. https://doi.org/10.1016/j.rser.2025.115694.
EC-2, 2010. Eurocode 2: Design of Concrete Structures. Part 1-1: General Rules and Rules for Buildings. CEN (European Committee for Standardization.
Ecoinvent Centre, 2024. Ecoinvent Database.
Euronorm, European Committee for Standardization, 2026. Rue De Stassart, 36, Belgium-1050 Brussels.
Fonte, R., Xydis, G., 2021. Wind turbine blade recycling: an evaluation of the European market potential for recycled composite materials. J. Environ. Manage. 287, 112269. https://doi.org/10.1016/j.jenvman.2021.112269.
Frazão, C., Barros, J., Bogas, J.A., García-Cortés, V., Valente, T., 2022. Technical and environmental potentialities of recycled steel fiber reinforced concrete for structural applications. J. Build. Eng. 45, 103579. https://doi.org/10.1016/j.jobe.2021.103579.
Global Wind Energy Council (GWEC), 2025. Global Wind Report 2025.
Güneyisi, E., Atewi, Y.R., Hasan, M.F., 2019. Fresh and rheological properties of glass fiber reinforced self-compacting concrete with nanosilica and fly ash blended. Constr. Build. Mater. 211, 349–362. https://doi.org/10.1016/j.conbuildmat.2019.03.087.
Guo, Y., Chen, S., Lakhiar, M.T., Chen, Q., Li, B., 2025. Effect of recycled turbine blade powder and fibres on mechanical and life cycle properties of mortar. Case Stud. Constr. Mater. 23, e05041. https://doi.org/10.1016/j.cscm.2025.e05041.
Henao, Y., Grubert, E., Korey, M., Bank, L.C., Gentry, R., 2024. Life cycle assessment and life cycle cost analysis of repurposing decommissioned wind turbine blades as high-voltage transmission Poles. J. Constr. Eng. Manage. 150 (5). https://doi.org/10.1061/JCEMD4.COENG-13718, 05024004-1.
Islam, M.J., Shahjalal, M., Haque, N.M.A., 2022. Mechanical and durability properties of concrete with recycled polypropylene waste plastic as a partial replacement of coarse aggregate. J. Build. Eng. 54, 104597. https://doi.org/10.1016/j.jobe.2022.104597.
Jang, E.S., Kang, C.W., 2022. Porosity analysis of three types of balsa (Ochroma pyramidale) wood depending on density. J. Wood Sci. 68 (1), 31. https://doi.org/10.1186/s10086-022-02037-2.
Jiang, C., Ng, C.T., Deng, M., Li, W., 2025. Debonding imaging in fibre reinforced concrete columns by deep learning assisted-guided wave technique. Mech. Syst. Signal Process. 240, 113409. https://doi.org/10.1016/j.ymssp.2025.113409.
Johst, P., Bühl, M., André, A., Kupfer, R., Protz, R., Modler, N., Böhm, R., 2025. Characterisation of end-of-life wind turbine blade components for structural repurposing: experimental and analytic prediction approach. Sustainability 17 (17), 7783. https://doi.org/10.3390/su17177783.
Jones, R., 1963. The ultrasonic testing of concrete. Ultrasonics 1 (2), 78–82. https://doi.org/10.1016/0041-624X(63)90058-1.
Joustra, J., Flipsen, B., Balkenende, R., 2021a. Structural reuse of wind turbine blades through segmentation. Compos. Part C: Open Access 5, 100137. https://doi.org/10.1016/j.jcomc.2021.100137.
Joustra, J., Flipsen, B., Balkenende, R., 2021b. Structural reuse of high end composite products: a design case study on wind turbine blades. Resour. Conserv. Recycl. 167, 105393. https://doi.org/10.1016/j.resconrec.2020.105393.
Kallenbacn, W., Groll, K., Herz, H., 2006. Concrete vs. plastic pipes decision criteria - planning - production - laying, Betonwerk Fertigteil Tech, 72 (2), 78–80.
Kumar, R., 2016. A comparative study on dry lean concrete manufactured with OPC vis-a-vis PPC to be used for the construction of concrete roads. Indian Concr. J. 90 (2), 70–76.
Li, J., Lin, G., Chen, X., 2025. Optimization of hierarchical groove–perforation structures in PET foam cores for wind turbine blade applications. Materials 18 (12), 2876. https://doi.org/10.3390/ma18122876.
Li, M., Xu, Z., Li, S., Kikuchi, Y., Dong, Y., Gryllias, K.C., Baraldi, P., Zio, E., Carroll, J., 2026. Health prognostics and maintenance decision-making for wind energy: a comprehensive overview. Renew. Sustain. Energy Rev. 226, 116269. https://doi.org/10.1016/j.rser.2025.116269.
Liu, K., Fan, H., Nie, L., Gu, J., Yuan, H., 2025a. Kinetics, product distribution and synergistic effects on the co-pyrolysis processes for epoxy resins and balsa wood. J. Anal. Appl. Pyrolysis 187, 106995. https://doi.org/10.1016/j.jaap.2025.106995.
Liu, X., Li, M., Wei, H., Tian, X., Ding, Y., 2025b. Axial compression performance of CFRP-confined lightweight aggregate concrete reinforced with hybrid fibers. J. Build. Eng. 113, 113972. https://doi.org/10.1016/j.jobe.2025.113972.
Liu, P., Barlow, C.Y., 2017. Wind turbine blade waste in 2050. Waste Manage. (Tucson, Ariz.) 62, 229–240. https://doi.org/10.1016/j.wasman.2017.02.007.
Manso-Morato, J., Hurtado-Alonso, N., Espinosa, A.B., Revilla-Cuesta, V., Ortega-López, V., 2026. Dimensional stability and water transport behavior of concrete with high contents of wind-turbine blade waste. Struct. Concr. 27 (1), 758–776. https://doi.org/10.1002/suco.70251.
Manso-Morato, J., Hurtado-Alonso, N., Revilla-Cuesta, V., Ortega-López, V., 2025b. Management of wind-turbine blade waste as high-content concrete addition: mechanical performance evaluation and life cycle assessment. J. Environ. Manage. 373, 123995. https://doi.org/10.1016/j.jenvman.2024.123995.
Manso-Morato, J., Hurtado-Alonso, N., Serrano-López, R., Revilla-Cuesta, V., Ortega-López, V., 2025c. Long-term mechanical performance of concrete with high amounts of wind turbine blade mixed waste: analysis of temporal evolution mechanisms. Case Stud. Constr. Mater. 23, e05194. https://doi.org/10.1016/j.cscm.2025.e05194.
Manso-Morato, J., Hurtado-Alonso, N., Skaf, M., Revilla-Cuesta, V., Ortega-López, V., 2025a. Life cycle assessment of concrete with wind turbine blade waste: a real case study. Environ. Impact Assess. Rev. 115, 107992. https://doi.org/10.1016/j.eiar.2025.107992.
Menna, C., De Simone, L., Capozzi, V., 2025. Mechanical recycling of GFRP wind turbine blades: evaluating the sustainability and economic potential of recycled fibers. Dev. Built Environ. 23, 100710. https://doi.org/10.1016/j.dibe.2025.100710.
Metha, P.K., Monteiro, P.J.M., 2014. Concrete: Microstructure, Properties and Materials, fourth ed. McGraw-Hill Education. 978-0-07-179787-0 (2014).
Mohamad, A.H.H., Ab-Rahim, R., 2025. Mapping the research landscape of energy market and renewable energy: a bibliometric analysis. Int. J. Renewable Energy Dev. 14 (4), 703–716. https://doi.org/10.61435/ijred.2025.61058.
Nagle, A.J., Mullally, G., Leahy, P.G., Dunphy, N.P., 2022. Life cycle assessment of the use of decommissioned wind blades in second life applications. J. Environ. Manage. 302, 113994. https://doi.org/10.1016/j.jenvman.2021.113994.
Ortega-López, V., Faleschini, F., Hurtado-Alonso, N., Manso-Morato, J., Revilla-Cuesta, V., 2024. Analysis of raw-crushed wind-turbine blade as an overall concrete addition: Stress–strain and deflection performance effects. Compos. Struct. 340, 118170. https://doi.org/10.1016/j.compstruct.2024.118170.
Pławecka, K., Przybyła, J., Korniejenko, K., Lin, W.T., Cheng, A., Łach, M., 2021. Recycling of mechanically ground wind turbine blades as filler in geopolymer composite. Materials 14 (21), 6539. https://doi.org/10.3390/ma14216539.
Pré Sustainability, Database and Support Teams, Simapro 9.5. What's New?, 2024.
Rafay, A., Irfan, M., Naqvi, S.R., Umer, M.A., Rehman, M.A., Saleem, M., Butt, M.S., Khan, A.U., 2024. Recovery and restoration of glass fibers from end-of-life composite waste through pyrolysis and partial oxidation processes combined with hot alkaline surface treatments. Polym. Compos. 45 (18), 16616–16629. https://doi.org/10.1002/pc.28916.
Ramaswamy, N., Joshi, B., Song, G., Mo, Y.L., 2025a. Residual mechanical properties of GFRP composites from decommissioned wind turbine blades for structural reuse. Compos. Struct. 374, 119739. https://doi.org/10.1016/j.compstruct.2025.119739.
Ramaswamy, N., Joshi, B., Song, G., Mo, Y.L., 2025b. Repurposing decommissioned wind turbine blades: a circular economy approach to sustainable resource management and infrastructure innovation. Renew. Sustain. Energy Rev. 215, 115629. https://doi.org/10.1016/j.rser.2025.115629.
Rani, M., Choudhary, P., Krishnan, V., Zafar, S., 2021. A review on recycling and reuse methods for carbon fiber/glass fiber composites waste from wind turbine blades. Compos. Part B: Eng. 215, 108768. https://doi.org/10.1016/j.compositesb.2021.108768.
Revilla-Cuesta, V., Faleschini, F., Pellegrino, C., Skaf, M., Ortega-López, V., 2024b. Water transport and porosity trends of concrete containing integral additions of raw-crushed wind-turbine blade. Dev. Built Environ. 17, 100374. https://doi.org/10.1016/j.dibe.2024.100374.
Revilla-Cuesta, V., Manso-Morato, J., Hurtado-Alonso, N., Skaf, M., Ortega-López, V., 2024a. Mechanical and environmental advantages of the revaluation of raw-crushed wind-turbine blades as a concrete component. J. Build. Eng. 82, 108383. https://doi.org/10.1016/j.jobe.2023.108383.
Revilla-Cuesta, V., Skaf, M., Ortega-López, V., Manso, J.M., 2023. Raw-crushed wind-turbine blade: waste characterization and suitability for use in concrete production. Resour. Conserv. Recycl. 198, 107160. https://doi.org/10.1016/j.resconrec.2023.107160.
Safaei, F., Tazi, N., Châtelet, E., Bouzidi, Y., 2022. When and how to repower energy systems? A four strategies-based decision model. ISA Trans. 125, 714–724. https://doi.org/10.1016/j.isatra.2021.08.006.
Shen, Y., Apraku, S.E., Zhu, Y., 2023. Recycling and recovery of fiber-reinforced polymer composites for end-of-life wind turbine blade management. Green Chem. 25 (23), 9644–9658. https://doi.org/10.1039/d3gc03479h.
Sim, S., Cho, S., Kim, G., Her, S., Jin, D., Bae, S., 2025. Exploring the impact of copper slag on the physicochemical properties of Portland limestone cement (PLC). J. Build. Eng. 101, 111964. https://doi.org/10.1016/j.jobe.2025.111964.
Tao, Y., Hadigheh, S.A., Wei, Y., 2023. Recycling of glass fibre reinforced polymer (GFRP) composite wastes in concrete: a critical review and cost benefit analysis. Structures 53, 1540–1556. https://doi.org/10.1016/j.istruc.2023.05.018.
Trento, D., Faleschini, F., Revilla-Cuesta, V., Ortega-López, V., 2024. Improving the early-age behavior of concrete containing coarse recycled aggregate with raw-crushed wind-turbine blade. J. Build. Eng. 92, 109815. https://doi.org/10.1016/j.jobe.2024.109815.
Vieira, T., Alves, A., de Brito, J., Correia, J.R., Silva, R.V., 2016. Durability-related performance of concrete containing fine recycled aggregates from crushed bricks and sanitary ware. Mater. Des. 90, 767–776. https://doi.org/10.1016/j.matdes.2015.11.023.
Wei, Y., Hadigheh, S.A., 2022. Cost benefit and life cycle analysis of CFRP and GFRP waste treatment methods. Constr. Build. Mater. 348, 128654. https://doi.org/10.1016/j.conbuildmat.2022.128654.
Wei, Y., Hadigheh, S.A., 2024. Enhancing carbon fibre recovery through optimised thermal recycling: kinetic analysis and operational parameter investigation. Mater. Today Sustainability 25, 100661. https://doi.org/10.1016/j.mtsust.2023.100661.
World Wind Energy Association (WWEA), 2025. WWEA Annual Report 2024: a Challenging Year for Windpower.

Wu, T., Wu, J., Zheng, C., Wang, J., 2024. Evaluation of freeze-thaw resistance of geopolymer concrete incorporating GFRP waste powder. J. Build. Eng. 90, 109465. https://doi.org/10.1016/j.jobe.2024.109465.

Xu, G.T., Liu, M.J., Xiang, Y., Fu, B., 2022. Valorization of macro fibers recycled from decommissioned turbine blades as discrete reinforcement in concrete. J. Clean. Prod. 379, 134550. https://doi.org/10.1016/j.jclepro.2022.134550.

Xu, M.X., Ji, H.W., Meng, X.X., Yang, J., Wu, Y.C., Di, J.Y., Jiang, H., Lu, Q., 2023. Effects of core materials on the evolution of products during the pyrolysis of end-of-life wind turbine blades. J. Anal. Appl. Pyrolysis 175, 106222. https://doi.org/10.1016/j.jaap.2023.106222.

Yazdanbakhsh, A., Bank, L.C., Rieder, K.A., Tian, Y., Chen, C., 2018. Concrete with discrete slender elements from mechanically recycled wind turbine blades. Resour. Conserv. Recycl. 128, 11–21. https://doi.org/10.1016/j.resconrec.2017.08.005.

Zhang, F., Lu, Z., Wang, D., 2024. Working and mechanical properties of waste glass fiber reinforced self-compacting recycled concrete. Constr. Build. Mater. 439, 137172. https://doi.org/10.1016/j.conbuildmat.2024.137172.